Interaction effects and energy barrier distribution on the magnetic relaxation of nanocrystalline hexagonal ferrites

X. Batlle,[*] M. García del Muro, and A. Labarta

Departament de Física Fonamental, Facultat de Física, Universitat de Barcelona, Diagonal 647, 08028 Barcelona, Catalonia, Spain
(Received 5 April 1996; revised manuscript received 29 October 1996)

The static and dynamic magnetic properties of nanocrystalline $BaFe_{10.4}Co_{0.8}Ti_{0.8}O_{19}$ M-type doped barium ferrite were studied in detail to clarify the effect of interactions on the magnetic relaxation of an assembly of small particles. The logarithmic approximation was unable to account for the magnetic relaxation of the sample. Interaction effects were analyzed from the low-field susceptibility, ΔM plots and the time dependence of thermoremanence, indicating that demagnetizing interactions led to an enhancement of both the relaxation rate at low temperatures and the amount of the lowest energy barriers. It is thus suggested that care should be taken when analyzing thermoremanent data at low temperature, in order not to confuse these experimental findings with the signature of macroscopic quantum tunneling. [S0163-1829(97)04709-7]

I. INTRODUCTION

Many experimental, theoretical, and numerical simulation studies have been devoted to the understanding of the magnetic relaxation of an assembly of small magnetic particles displaying an effective energy barrier distribution, arising, for example, from a particle volume distribution and/or an anisotropy field distribution and from interparticle interactions.[1] This subject is still not fully resolved. It is both important to basic research and relevant to the magnetic recording industry since it determines the average lifetime of magnetic recording media.[2] Some of us[3] showed recently that time-dependent thermoremanence data for small particle systems collapse onto a single master curve with the scaling variable $T \ln(t/\tau_0)$. It was also shown that, within the scope of this procedure, the effective distribution of energy barriers might be obtained from the experimental master curve.[4] In addition, numerical simulation studies suggested that an enhancement in the amount of the lowest energy barriers existed if dipolar interparticle interactions were demagnetizing.[5] These results were relevant when considering what is known as quantum tunneling of the magnetization.[6]

In order to ascertain the effect of interactions on the magnetic relaxation of an assembly of small particles, a study of the magnetic properties of nanocrystalline $BaFe_{10.4}Co_{0.8}Ti_{0.8}O_{19}$ M-type doped barium ferrite was carried out. The aim of this work was to experimentally show that demagnetizing interactions might lead to an enhancement of both the amount of the lowest energy barriers and the relaxation rate at low temperatures.

M-type barium ferrites have been studied for a long time because of their technological applications,[7] as well as for their great pure research interest.[7–12] From the magnetic point of view, pure M-type barium ferrite $BaFe_{12}O_{19}$ and related compounds obtained by cationic substitution, display a large variety of magnetic structures, from collinear ferrimagnetism[8,9] to canonic spin-glass-like behavior,[12] which depend on the degree of magnetic frustration induced by cationic substitution. In particular, the $BaFe_{10.4}Co_{0.8}Ti_{0.8}O_{19}$ compound seems to be ideal for per-

pendicular magnetic recording.[9,13–15] In order to observe thermal relaxation effects on this compound at about and below room temperature, particles of about 30 nm must be obtained. The glass crystallization method (GCM)[15,16] appears to be particularly successful in controlling particle size, from the microcrystalline region (microns) to the nanocrystalline regime (nanometers). It has proved to be an excellent method of obtaining M-type doped barium ferrite nanocrystalline powders with sizes of about 10 nm (depending on both the thermal treatment and the doping cations). These have a plateletlike shape and a narrow size distribution.[11,15,17]

II. EXPERIMENTAL

Nanocrystalline $BaFe_{10.4}Co_{0.8}Ti_{0.8}O_{19}$ particles were prepared by the glass crystallization method.[15,16] X-ray-diffraction (XRD) data[18] showed very broad peaks and the fitting of the whole spectra to the M-type structure demonstrated the plateletlike morphology of the particles, leading to a mean particle diameter $\bar{D} = (7.6 \pm 2.4)$ nm, a mean thickness $\bar{t} = (2.4 \pm 0.7)$ nm, and a mean particle volume $\bar{V} \simeq 90$ nm^3. Transmission electron microscopy (TEM) also showed the plateletlike morphology[17] and a certain degree of preferential orientation:[17,19,20] particles tended to pile up and produce stacks along the perpendicular direction to the (001) face of the platelet, which corresponds to the easy axis.[8,9] Particle clusters were also observed.[19,21] TEM studies led to a lognormal distribution of particle sizes, with a mean diameter of about 10.2 nm and a mean volume of about 105 nm^3. We note that the cell parameters of the hexagonal unit cell of $BaFe_{12}O_{19}$ are $a \simeq 0.589$ nm and $c \simeq 2.32$ nm (see Ref. 8).

That degree of preferential orientation is a consequence of the diameter of the (001) face being much larger than the platelet thickness. Interactions were expected to be magnetizing among particles within the same stack[20,22,23] and demagnetizing among the stacks and within particle clusters.[21–23] Both types of interactions are always present in barium ferrites but one is dominant.
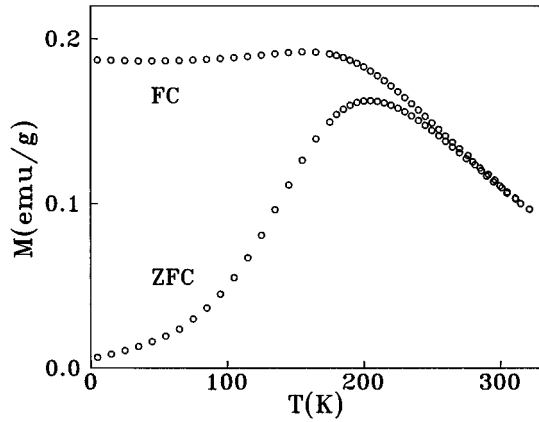
FIG. 1. Zero-field-cooling and field-cooling magnetizations as a function of temperature measured at 35 Oe.

FIG. 2. Saturation magnetization M_s as a function of temperature measured at 50 kOe. The solid line corresponds to the best fit of data to Eq. (1). Inset: log-log plot of $[M_1 - M_s(T)]$ as a function of temperature, where $M_1 = M_s$ (15 K). The straight line corresponds to the best linear fit of the data, with a slope $\alpha = 1.75$, indicating that the terms $T^{3/2}$ and $T^{5/2}$ should be considered when fitting M_s to Eq. (1).

Low-field susceptibility at 35 Oe and isothermal magnetization up to 50 kOe were recorded in the range 5–325 K. The time dependence of the thermoremanence was measured at various temperatures (27 temperatures within 9–230 K) by field cooling the sample at 200 Oe from room temperature down to the measuring temperature and then switching off the field. The field dependence of both the isothermal remanent magnetization and the dc demagnetizing remanence was carried out up to 50 kOe. All magnetic measurements were recorded with a SQUID magnetometer for particles which had been fixed with a glue in a plastic substrate in order to avoid particle rotation towards the field axis.

III. MAGNETIC CHARACTERIZATION

The zero-field-cooling (ZFC) and field-cooling (FC) curves displayed all the typical features of an assembly of small magnetic particles with a distribution of energy barriers (Fig. 1). The ZFC curve showed a wide maximum at about $T_M = 205 \pm 5$ K and both curves tended to be superimposed at above $T_{irr} \simeq 285$ K, as the superparamagnetic (SPM) regime was reached. The fact that the FC curve was very flat below about T_M, in comparison with noninteracting small particle systems, suggested the existence of magnetic interactions among particles. Then, T_M reflected both blocking and freezing processes, the latter due to interactions.

The temperature dependence of the saturation magnetization M_s was measured at 50 kOe (Fig. 2) and may be attributed essentially to spin wave excitation. The thermal dependence of M_s was fitted to the following demagnetizing law:

$$M_s(T) = M_s(0)(1 - BT^{3/2} - ET^{5/2}), \qquad (1)$$

Figure 2 shows the best fit of data to Eq. (1) within the range 60–300 K, leading to $B = 4.1(1) \times 10^{-5}$ K$^{-3/2}$ and $E = 3.7(2) \times 10^{-8}$ K$^{-5/2}$. The $T^{3/2}$ term was the dominant demagnetizing mechanism in the whole temperature range. However, the fitted value for B is about one order of magnitude higher than those values corresponding to bulk samples,[24–26] as a consequence of the finite-size effects arising from both the cutoff in the large wave vectors of the spin-wave spectra and the characteristic surface excitations.

The blocking temperature distribution $F(T_B)$ was obtained by fitting the temperature derivative of the remanent-to-saturation magnetization ratio (maximum applied field of 50 kOe) to a log-normal distribution. The fitted values were the following: $T_{B0} = 81$ K (peak of the distribution), $\overline{T}_B = 86$ K (mean blocking temperature) and $\sigma = 0.38$ [half width of the $\ln(\overline{T}_B)$ distribution].[11] The same log-normal distribution of volumes was found by fitting the magnetization curves in the SPM regime to a distribution of Langevin function.[27]

The low-field susceptibility of an assembly of interacting particles in the SPM regime is expected to be of the form

$$\chi \sim \frac{\overline{\mu}^2}{3 k_B (T - T_0)}, \qquad (2)$$

where $\overline{\mu}$ is the mean magnetic moment per particle and T_0 arises from the interparticle interactions. The reciprocal of the FC data is shown in Fig. 3, where the y axis was multiplied by $m_s^2(T) = M_s^2(T)/M_s^2(0)$ in order to correct the temperature dependence of $\overline{\mu}$ in Eq. (2). The extrapolated value of T_0 was obtained by fitting the data to Eq. (2) and was found to be -170 ± 30 K, suggesting that interactions were demagnetizing in the SPM regime. As noted in Ref. 28, this interaction temperature could be considerably affected by the progressive blocking of the particles. However, in the present case, the linearity of the reciprocal susceptibility was lost below about 275 K, while at this temperature the blocking temperature distribution was nearly zero [$F(275K)/F(\overline{T}_B) = 6 \times 10^{-3}$]. Therefore, the contribution of the progressive blocking to T_0 was very small.

Using the measured value for M_{FC}/H at 300 K and the corresponding bulk saturation magnetization for this material [$M_b(300$ K$) = 317$ emu/cm^3],[8,9] a mean magnetic volume $\overline{V}_m$ of the order of 36 nm^3 was found from Eq. (2), assuming that $\overline{\mu} = M_b \overline{V}_m$. Other $\overline{V}_m$ values achieved from various
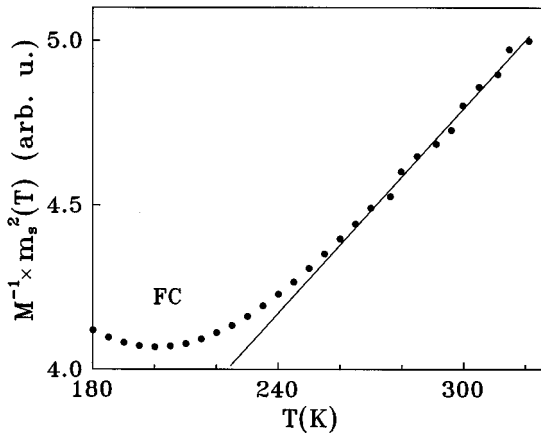
FIG. 3. Detail of the reciprocal of the field-cooling magnetization as a function of temperature. The y axis has been multiplied by $m_s^2(T)$ in order to correct the temperature dependence of $\bar{\mu}$ in Eq. (2) (see text).

techniques[23,27] were also smaller than those obtained by TEM (105 nm^3) and XRD (90 nm^3), as expected due to surface magnetic effects.[10]

Two different primary curves concerning the field dependence of the remanence were measured:[29] (1) the isothermal remanent magnetization curve $m_r(H) = M_r(H)/M_r(H_{max})$, which was obtained measuring the remanence from the initially demagnetized state and taking the sample through progressively increasing loops; and (2) the dc demagnetizing remanence curve $m_d(H) = M_d(H)/M_d(H_{max})$, which was obtained measuring the remanence by progressively increasing demagnetization in a previously saturated sample. Both remanence curves are expected to be related in non-interacting systems as[30]

$$m_d(H) = 1 - 2m_r(H), \quad (3)$$

Equation (3) assumes that magnetizing and demagnetizing processes are equivalent, which implies that deviations from linearity in a plot of $m_d(H)$ vs $m_r(H)$ (Henkel plots)[31] arise due to interactions. A qualitative measure of the sign and strength of interactions may be achieved by representing $\Delta M = m_d(H) - [1 - 2m_r(H)]$ as a function of the field.[32] $\Delta M < 0$ suggests that interactions are demagnetizing while $\Delta M > 0$ suggests that interactions are magnetizing. The ΔM plot (Fig. 4) indicates that interactions are demagnetizing in the blocked regime, in agreement with what was found in the SPM regime (Fig. 3). In the blocked regime, the magnetization vectors are pinned to the easy axis of the particles. Within a given stack, the parallel arrangement is the stable configuration, while between different stacks the stable one is the antiparallel configuration. Concerning particle clusters, such as, for example, quasispherical aggregates, the overall configuration favors demagnetization.[20–23]

According to Eq. (3), $|dm_d/dH| = 2dm_r/dH$. If deviations from this relationship may be attributed to interparticle interactions, an order of magnitude of the mean interaction field H_{int} might be obtained as[31,33] $H_{int} \simeq 1/2(H_r' - H_r)$, where H_r and H_r' correspond to the position of the maxima of the field derivative of the m_r and m_d curves, respectively. Figure 5 shows that $H_r > H_r'$ suggesting that interactions
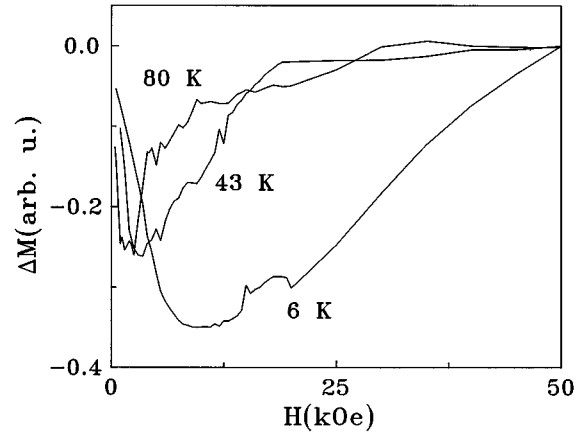
FIG. 4. ΔM plots [$\Delta M = m_d(H) - (1 - 2m_r(H))$], showing demagnetizing interactions in the blocked regime.

were demagnetizing in the blocked regime, and H_{int} is about 1.2 kOe.

Finally, the mean value of the anisotropy field was found to be $H_a(5 \text{ K}) \simeq 18$ kOe, taking into account that the anisotropy field distribution is proportional to dm_r/dH and removing the effect of the thermal fluctuations of the SPM particles.[33] This value is much higher than that corresponding to microcrystalline particles of the same composition [$H_a(5 \text{ K}) \simeq 6$ kOe for particles with a mean volume[33] of 20×10^3 nm^3] as has been previously found in other nanoparticulate systems.[25]

IV. THERMOREMANENT MAGNETIZATION: $T \ln(t/\tau_0)$ SCALING

The time dependence of the thermoremanence was analyzed in terms of the $T \ln(t/\tau_0)$ scaling with $\tau_0 = 10^{-12}$ s (Fig. 7): it was recently shown by some of us that the magnitude $T \ln(t/\tau_0)$ behaved as the scaling variable for the time relaxation of the magnetization (see Ref. 3 and references therein). As a result of the scaling, a single master curve that stands for the whole relaxation curve at the lowest measuring temperature (9 K) is obtained, at times as high as 10^{374} s. Figures 6 and 7 show that what is known as the logarithmic
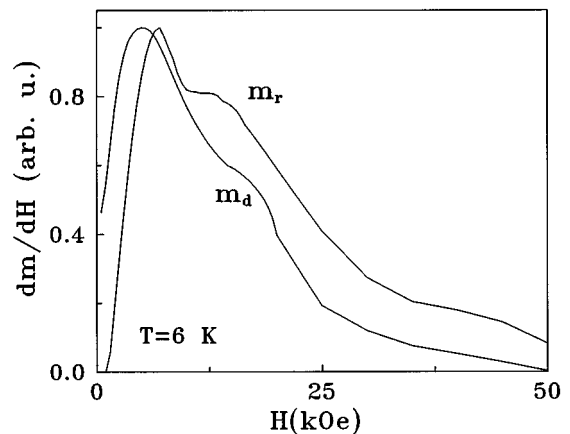
FIG. 5. Derivatives of $m_r(H)$ and $m_d(H)$ with respect to the applied magnetic field at 6 K.
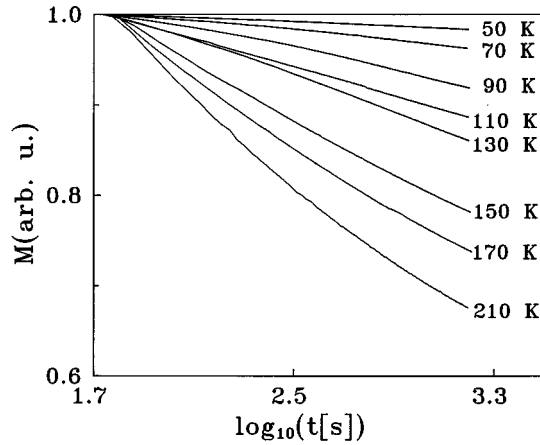
FIG. 6. Thermoremanent magnetization [normalized to $M(t=0,T)$], plotted as a function of $\log_{10}(t)$ at various temperatures within 9 and 210 K.

approximation is only valid around the inflection point of the master curve, which, at each given temperature, corresponds to the time window at which those energy barriers near the maximum of the distribution function are relaxing.

In order to reproduce the experimental master curve, we assume that the time decay of the magnetization arises from a single log-normal distribution of energy barriers $f(E)$ and may be expressed as[1,33]

$$M(t) = M_0 \int_0^\infty dE f(E) e^{-t/\tau(E)}, \tag{4}$$

where $\tau(E)$ is the relaxation time given by the Arrhenius law used in Néel's theory.[34] We have fitted the experimental master curve to Eq. (4) by numerical calculation of the integral, with three fitting parameters: the blocking temperature T_{B0} associated with the energy E_0 corresponding to the peak of the distribution [$T_{B0} = E_0/(32k_B)$], the half width of the distribution σ, and $M_0 = M(H=0, t=0)$. We have found
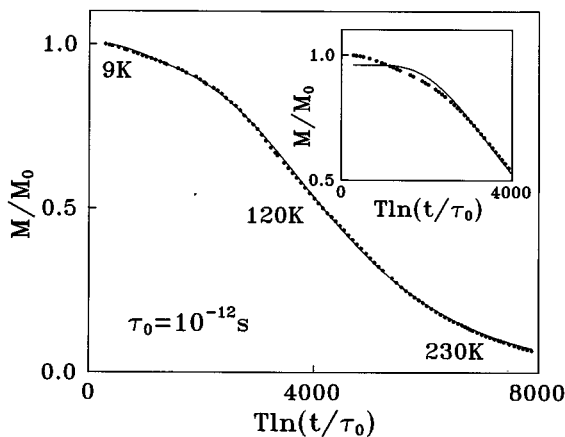
FIG. 7. M/M_0 vs $T \ln(t/\tau_0)$ scaling with $\tau_0 = 10^{-12}$ s for 27 temperatures within 9 and 230 K. Solid line represents the best fit of data to Eq. (4) considering two log-normal distributions of energy barriers: $f(E) = [p f_1(E) + (1-p) f_2(E)]$. Inset: Detail of the plot of the same data within 9 and 120 K. Solid line represents the best fit of data to Eq. (4), assuming a single log-normal distribution.
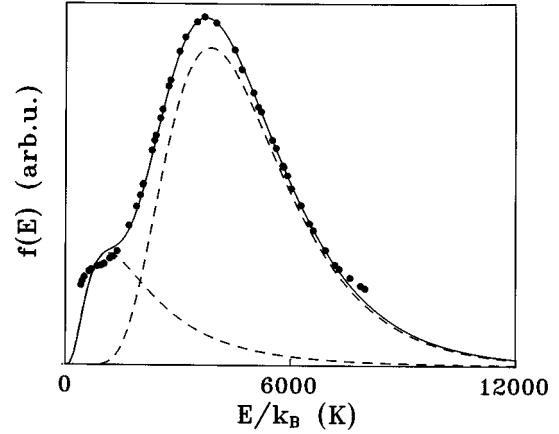
FIG. 8. Energy barrier distribution: (dashed lines) lognormal distributions $p f_1(E)$ and $(1-p) f_2(E)$ obtained from the fitting of the experimental master curve M/M_0 vs $T \ln(t/\tau_0)$ to Eq. (4); (solid line) $f(E) = [p f_1(E) + (1-p) f_2(E)]$; Filled circles correspond to the derivative of the experimental master curve with respect to the scaling variable.

that large discrepancies appear at low temperatures (see inset of Fig. 7), where the slope of the experimental curve is higher than that of the fitted curve, denoting that the relaxation rate at low temperatures is larger than that expected for a single log-normal distribution.

It was shown by both theoretical arguments and experimental results (see Ref. 4, and references therein) that, within the scope of the $T \ln(t/\tau_0)$ procedure, the effective distribution of energy barriers may be obtained from the experimental master curve by calculating the derivative of this curve with respect to $T \ln(t/\tau_0)$. Figure 8 displays this derivative, where an enhancement of the amount of the lowest energy barriers is evident. Numerical simulation[5] showed that demagnetizing interactions act to favor relaxation at low temperatures, leading to an enhancement of the relative contribution of the lowest energy barriers and to a displacement of the whole distribution towards the origin. As this energy density arises from the volume and anisotropy distributions and from the interparticle interactions, it is not possible to separate the enhancement due to demagnetizing interactions from that due to the existence of very small particles. However, the fluctuation field analysis[23] evidences that both the activation volume and the low-energy contribution increase with demagnetizing interactions. Taking into account these results and the fact that we have found that the overall interactions are demagnetizing in this sample, we assume that the observed extra contribution may be mainly due to the effect of the demagnetizing interactions. In order to account for it, the fitting of the master curve has been done by considering two log-normal distributions of energy barriers, $f_1(E)$ and $f_2(E)$, so as that the total energy barrier distribution is $f(E) = [p f_1(E) + (1-p) f_2(E)]$, where p is the relative weight.

A good fit is obtained (Fig. 7) with the following parameters: $T_{B01} = 38$ K, $T_{B02} = 121$ K, $\sigma_1 = 0.74$, $\sigma_2 = 0.40$ and $p = 0.19$. $f_1(E)$ describes the extra contribution to the lowest energy barriers, while $f_2(E)$ is centered at high energies and describes the contribution of non or weakly interacting particles and/or particles with magnetizing interactions (which

shifts energy to higher values). As p is much lower than 1, the effective distribution of energy barriers $f(E)$ is dominated essentially by $f_2(E)$ so that the high temperature relaxation measurements, remanent-to-saturation data,[11] and the isothermal magnetization curves in the SPM regime[27] may be accurately described by taking into consideration a single log-normal distribution. The fitted value of σ_2 is in reasonable agreement with that obtained from thermoremanent data ($\sigma = 0.38$), while T_{B02} lies in between the peak of the blocking temperature distribution (81 K) and the maximum of the ZFC ($T_M = 205$ K), as found in other particulate systems.[3,4] Moreover, the total distribution function obtained from the fitting $f(E)$ perfectly matches the effective distribution of energy barriers obtained from the derivative of the experimental master curve (see Fig. 8).

Finally, let us show that dipolar interactions may account for these experimental features. An order of magnitude of the overall demagnetizing dipolar field H_{int} may be gained from the shift towards the origin (ΔE) of the maximum of $f(E)$ with respect to that corresponding to $f_2(E)$, since the former stands for the effective distribution that takes into account the net dipolar interactions and we assume that the latter corresponds to those energy barriers non or weakly modified by the dipolar interactions. Then, $H_{int} \simeq \Delta E / \bar{\mu} = 1.1$ kOe, where $\Delta E / k_B \simeq 134$ K and $\bar{\mu}(4.2 \text{ K}) = M_b(4.2 \text{ K})\bar{V}_m$; $[M_b(4.2 \text{ K}) = 475.2 \text{ emu/cm}^3]$.[8,9] This value is in close agreement with that obtained from the field dependence of the remanence (see Fig. 5; $H_{int} = 1.2$ kOe). Both values of H_{int} are also in agreement with a rough estimation of the maximum dipolar field that a mean particle senses due to a nearest-neighboring mean particle (two particles which are stacked along the c axis): assuming a point-dipole model, $H_{int}^{max} \simeq 2\bar{\mu}/\bar{t}^3 = 2.5$ kOe. We note that $\Delta E / k_B$ is of the order of T_0, and both values are about one order of magnitude larger than those found in other fine particle systems.[28,35]

giving place to very large dipolar fields, which is probably due to particle aggregation. These high values of the dipolar fields are responsible for the *anomalous* energy barrier distribution of this sample.

Summarizing, we have experimentally shown that an increase in the low-energy barrier density exists in an assembly of $BaFe_{10.4}Co_{0.8}Ti_{0.8}O_{19}$ nanocrystalline particles and this fact may be attributed to the effect of the dominant demagnetizing interactions, although the presence of very small particles cannot be precluded. Therefore, care should be taken when analyzing the relaxation data in order to ascertain which are the relaxation mechanisms, since an enhancement of the relaxation rate at very low temperatures, similar to that described in this paper, may be wrongly attributed to macroscopic quantum tunneling. We would also like to stress the fact that the $T \ln(t/\tau_0)$ scaling procedure is a useful method to obtain the effective distribution of energy barriers without making any *a priori* assumption about $f(E)$, even in those situations in which dipolar interactions among particles are relevant.

*Author to whom correspondence should be sent. Electronic address: xavier@littlefly.ffn.ub.es

[1] R. Street and J. C. Wooley, Proc. Phys. Soc. London A **62**, 562 (1949); C. P. Bean and J. D. Livingston, J. Appl. Phys. **30**, 120S (1959); E. P. Wohlfarth, J. Phys. F **14**, L155 (1984); K. O'Grady, A. Bradbury, J. Popplewell, S. W. Charles, and R. W. Chartrell, J. Magn. Magn. Mater. **49**, 106 (1985); R. Street, R. K. Day, and J. B. Dunlop, *ibid.* **69**, 106 (1987); A. M. de Witte, K. O'Grady, G. N. Coverdale, and R. W. Chantrell, *ibid.* **88**, 183 (1990); for a review see, R. W. Chantrell, *ibid.* **95**, 365 (1991); R. Street, P. G. Mc Cormick and L. Folks, *ibid.* **104-107**, 368 (1992); R. W. Chantrell, A. Liberatos, M. El-Hilo, and K. O'Grady, J. Appl. Phys. **76**, 6409 (1994).

[2] See, for example, P. J. Flanders and M. P. Sharrock, J. Appl. Phys. **62**, 2918 (1987), and references therein.

[3] A. Labarta, O. Iglesias, Ll. Balcells, and F. Badía, Phys. Rev. B **48**, 10 240 (1993). See, for spin glasses, J. J. Préjean and J. Souletie, J. Phys. (France) I **41**, 1335 (1980); R. Omari, J.J. Préjean, and J. Souletie, *ibid.* **45**, 1809 (1984).

[4] O. Iglesias, F. Badía, A. Labarta, and Ll. Balcells, J. Magn. Magn. Mater. **140-144**, 399 (1995); Z. Phys. B **100**, 173 (1996).

[5] R. Ribas and A. Labarta, J. Magn. Magn. Mater. **157-58**, 351 (1996); J. Appl. Phys. **80**, 5192 (1996).

[6] M. Uehara and B. Barbara, J. Phys. (France) **47**, 235 (1986), E.

Chudnovsky and L. Gunter, Phys. Rev. Lett. **60**, 661 (1988); X. X. Zhang, Ll. Balcells, J. M. Ruiz, O. Iglesias, and J. Tejada, Phys. Lett. A **163**, 130 (1992); J. I. Arnaudas, A. Del Moral, C. de la Fuente, and P. A. J. de Groot, Phys. Rev. B **47**, 11 924 (1993).

[7] M. P. Sharrock and L. Josephson, IEEE Trans. Magn. **MAG-22**, 723 (1986); T. Fujiwara, *ibid.* **MAG-23**, 3125 (1987); M. P. Sharrock, *ibid.* **MAG-25**, 4374 (1989); M. H. Kryder, J. Magn. Magn. Mater. **83**, 1 (1990).

[8] H. Kojima, in *Ferromagnetic Materials*, edited by E. P. Wohlfarth (North-Holland, Amsterdam, 1982), Vol. 3; J. Smith and H. P. Wijn, in *Ferrites* (Philips Technical Library, Eindhoven, 1960); E. W. Gorter, Proc. IEEE **104B**, 225 (1957).

[9] X. Batlle, X. Obradors, J. Rodríguez-Carvajal, M. Pernet, M. V. Cabañas, and M. Vallet, J. Appl. Phys. **70**, 1614 (1991), and references therein.

[10] X. Batlle, X. Obradors, M. Medarde, J. Rodríguez-Carvajal, M. Pernet, and M. Vallet, J. Magn. Magn. Mater. **124**, 228 (1993), and references therein.

[11] X. Batlle, M. García del Muro, J. Tejada, H. Pfeiffer, P. Görnert, and E. Sinn, J. Appl. Phys. **74**, 3333 (1993).

[12] A. Labarta, X. Batlle, B. Martínez, and X. Obradors, Phys. Rev. B **46**, 8994 (1992); X. Batlle, A. Labarta, B. Martínez, X. Obra-

dors, M. V. Cabañas, and M. Vallet, J. Appl. Phys. **70**, 6172 (1991).

[13] Japan Technology Highlights, Vol. 2, No. 20 (1991).

[14] O. Kubo, T. Ido, and H. Yokoyama, IEEE Trans. Magn. **MAG-18**, 1112 (1982); O. Kubo, T. Ido, H. Yokoyama, and Y. Koike, J. Appl. Phys. **57**, 4280 (1985).

[15] P. Görnert, E. Sinn, and M. Rösler, Key Eng. Mater. **58**, 129 (1991); P. Görnert, E. Sinn, W. Schüppel, H. Pfeiffer, M. Rösler, Th. Schubert, M. Jurisch, and R. Sellger, IEEE Trans. Magn. **MAG-26**, 12 (1990); M. Rösler, P. Görnert, and E. Sinn, Z. Phys. D **19**, 279 (1991).

[16] B. T. Shirk and W. R. Buessem, J. Am. Ceram. Soc. **53**, 192 (1970).

[17] P. Görnert, H. Pfeiffer, E. Sinn, R. Müller, W. Shüppel, M. Rösler, X. Batlle, M. García del Muro, J. Tejada, and S. Galí, IEEE Trans. Magn. **MAG-30**, 714 (1994).

[18] S. Galí (private communication).

[19] T. Ido, O. Kubo, and H. Yokoyama, IEEE Trans. Magn. **MAG-22**, 704 (1986).

[20] P. I. Mayo, R. M. Erkkila, A. Bradbury, and R. W. Chantrell, IEEE Trans. Magn. **MAG-26**, 1894 (1990).

[21] M. El-Hilo, K. O' Grady, and R. W. Chantrell, IEEE Trans. Magn. **MAG-27**, 4666 (1991).

[22] M. El-Hilo, H. Pfeiffer, K. O'Grady, W. Schüppel, E. Sinn, P. Görnert, M. Rösler, D. P. E. Dickson, and R. W. Chantrell, J. Magn. Magn. Mater. **129**, 339 (1994).

[23] M. García del Muro, X. Batlle, A. Labarta, J.M. González, and M. I. Montero, J. Appl. Phys. (to be published).

[24] C. Djega-Mariadassou, J. L. Dormann, M. Noguès, G. Villers, and S. Sayouri, IEEE Trans. Magn. **MAG-26**, 1819 (1990); J. L. Dormann, M. Noguès, and J. Jové, J. Magn. Magn. Mater. **104-107**, 1567 (1992).

[25] See, for example, *Magnetic Properties of Fine Particles*, edited by J. L. Dormann and D. Fiorani (North-Holland, Amsterdam, 1992).

[26] *Science and Technology of Nanostructured Magnetic Materials*, edited by G. C. Hadjipanayis and G. A. Prinz (Pleum Press, New York, 1991).

[27] X. Batlle, M. García del Muro, A. Labarta, and P. Görnert, J. Magn. Magn. Mater. **157-58**, 191 (1996); X. Batlle, M. García del Muro, and A. Labarta (unpublished).

[28] M. El-Hilo, K. O' Grady, and R. W. Chantrell, J. Magn. Magn. Mater. **117**, 21 (1992).

[29] See, K. O'Grady and R. W. Chantrell, in *Magnetic Properties of Fine Particles* (Ref. 25), p. 93.

[30] E. P. Wohlfarth, J. Appl. Phys. **29**, 595 (1958).

[31] O. Henkel, Phys. Status Solidi **7**, 919 (1974); G. W. D. Spratt, P. R. Bissell, R. W. Chantrell, and E. P. Wohlfarth, J. Magn. Magn. Mater. **75**, 309 (1988).

[32] P. E. Kelly, K. O'Grady, P. I. Mayo, and R. W. Chantrell, IEEE Trans. Magn. **MAG-25**, 3881 (1989).

[33] H. Pfeiffer, Phys. Status Solidi A **118**, 295 (1990); H. Pfeiffer and W. Schüppel, *ibid.* **119**, 259 (1990), H. Pfeiffer, *ibid.* **120**, 233 (1990).

[34] L. Néel, Ann. Geophys. **5**, 99 (1949).

[35] T. Jonsson, J. Mattsson, C. Djurberg, F. A. Khan, P. Nordblad, and P. Svedlindh, Phys. Rev. Lett. **75**, 4138 (1995).